Commun. Comput. Phys.
doi: 10.4208/cicp.160313.290813a

Vol. **15**, No. 3, pp. 677-691
March 2014

Investigating Plasma Jets Behavior using Axisymmetric Lattice Boltzmann Model under Temperature Dependent Viscosity

Ridha Djebali*

ISLAIB – Béja 9000, University of Jendouba, Tunisia.

Received 16 March 2013; Accepted (in revised version) 29 August 2013

Communicated by Xueqiao Xu

Available online 1 November 2013

Abstract. This study aims to investigate turbulent plasma flow using the lattice Boltzmann (LB) method. A double population model D2Q9-D2Q4 is employed to calculate the plasma velocity and temperature fields. Along with the calculation process a conversion procedure is made between the LB and the physical unit systems, so that thermo-physical properties variation is fully accounted for and the convergence is checked in physical space. The configuration domain and the boundary condition treatment are selected based on the most cited studies in order to illustrate a realistic situation. The jet morphology analysis gives credible results by comparison with commonly published works. It was demonstrated also that accounting for the substrate as wall boundary condition modify greatly the flow and temperature structures with may affect absolutely the particles behavior during its in-flight in the hot gas.

AMS subject classifications: 35Q20, 35Q30, 76F65, 80M25, 81T80, 82D10, 82C80, 82C70

Key words: LB method, axisymmetric model, temperature dependent viscosity, turbulence, plasma jets.

1 Introduction

Surfaces coating by plasma spraying is an important manufacturing process with many industrial applications. In the last several decades, numerical modeling of plasma spraying processes has met with considerable attention [1–3]. That is in order to well understand the complex phenomena the plasma spray involves, for economic constraints and to well predict the plasma-inflight-particles exchanges since this affects directly the coating formability and microstructure. Plasma jets have been very successful in many

*Corresponding author. *Email address:* ridha.djebali@ipein.rnu.tn (R. Djebali)

applications such as spraying, cutting, welding,$\cdots$. The excellent choice of high performance plasma gases and spraying materials has been the subject of several experimental and numerical efforts. An excellent choice will be the response of efficient numerical studies and the results of experimental tests. However, plasma jets are high temperature flows (>8000K); therefore, all diffusion parameters involved in conservation equations are temperature dependent.

This study deals with the investigation of plasma jets using an axisymmetric LB thermal model. We use in the following the axisymmetric formulation based on the J. G. Zhou's model [4].

2 Mathematical considerations

In conventional CFD methods, the conservation equations of macroscopic quantities are discretized to generally up-to second order, which leads to complex algebraic equations. However, in lattice Boltzmann method, the fluid consists of fictive particles that move in consecutive collision – streaming processes over a discrete lattice mesh. Due to its particulate nature, this approach has met with particular interest from researchers and has become a powerful tool in CFD modeling. In other side, jet flows form an important field for scientific research and industrial applications. The jet flows presents some specificity related to its discharging behaviour, in addition to the complexities of treating the boundary conditions for numerical studies. Plasma jets fall into this category and a special treatment is needed due to the high temperature (>8000K) and high velocity fields.

2.1 Continuum governing equations

The continuity, momentum and energy equations governing an incompressible axisymmetric plasma jet flow in (z,r) coordinates are written in tensorial form as follows in the Eq. (2.1):

$$\begin{cases} \partial_j u_j = -u_r/r, \\ \partial_t u_i + u_j \partial_j \partial u_i = -\partial_i p/\rho + v\left(\partial_j^2 u_i + \partial_r u_i/r - u_i \delta_{ir}/r^2\right), \\ \partial_t \theta + u_j \partial_j \theta = \alpha\left(\partial_j^2 \theta + \partial_r \theta/r\right), \end{cases} \tag{2.1}$$

where t is the time, (u_r,u_z) are the radial and axial velocity components, ρ is the fluid density, θ is the dimensionless gas temperature, v is the kinetic viscosity, α is the thermal diffusivity, p is the pressure and δ_{ir} is the Kronecker delta symbol.

2.2 Lattice Boltzmann approach

The lattice Boltzmann (LB) method was proposed a decade ago [5–7] and has been developed to offer an alternative numerical tool to conventional Computational Fluid Dynamics (CFD) for simulating fluid flows. The LB classical collision model (BGK) was

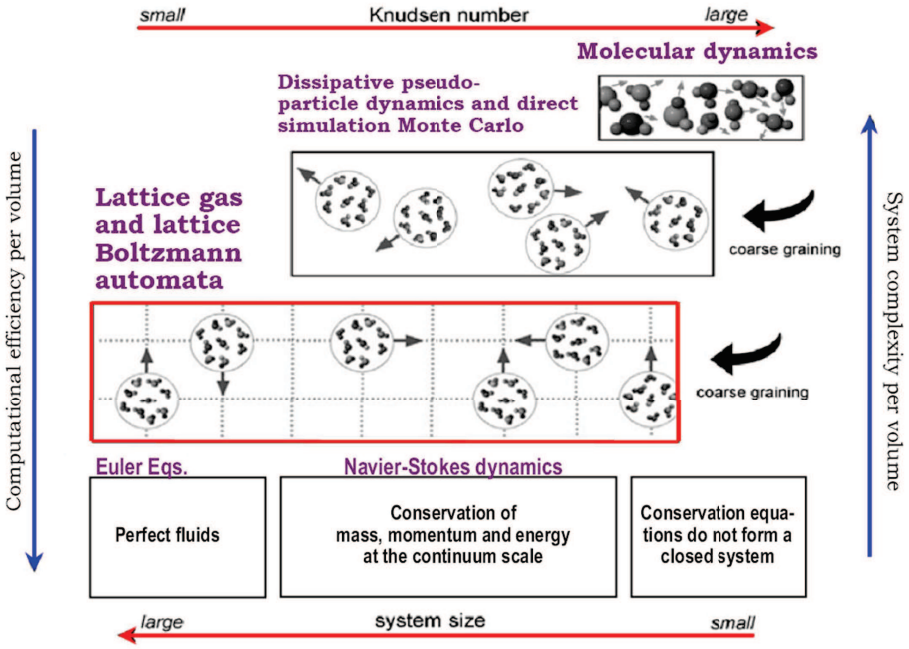

Figure 1: Positioning the LB methods relative to the commonly used computational fluid dynamics approaches gathered with their applicability ranges ([13] with revisions).

introduced to overcome the drawbacks and shortcomings of its ancestor, the lattice gas cellular automata (LGCA) method. Unlike conventional methods based on a macroscopic continuum equation, the LB method starts from mesoscopic kinetic equation of the Boltzmann equation, to determine macroscopic fluid dynamics. The macroscopic fluid dynamics emerge from the causal dynamics of a fictitious ensemble of particles, whose motion and interactions are confined to a regular space-time lattice (see Fig. 1). The kinetic nature brings certain advantages over conventional numerical methods, as natural for parallel computing, easy handling of complex geometries, particle-based method, only density distribution function $f_k(\vec{x},t)$ as dependent variable, algebraic operation, a large range of applicability (from microscopic to macroscopic scales). The LBM has the beneficial feature of simulating complex fluid flows such as multiphase flows [8, 9], multicomponents [10] flows, porous media flows [3], flows with suspensions [11] and compressible flows [12].

Recently some axisymmetric models for simulating fluid flow have been developed. The Zhou's model [4] will be used in this work. The proposed LB model can be written, for the nine-velocity directions $0 \leq k \leq 8$, as follows:

$$f_k(\vec{x}+\Delta\vec{x},t+\Delta t)-f_k(\vec{x},t)=-\frac{1}{\tau_v}\left[f_k(\vec{x},t)-f_k^{eq}(\vec{x},t)\right]+\Delta t F_1+\frac{\Delta t}{6}e_{ki}F_{2i}, \tag{2.2}$$

where Δt is lattice time unit, $\vec{x}$ is the lattice site, f_k is the density distribution function and

$F_1=-\rho u_r/9r$ and $F_{2i}=-\rho[u_iu_r/r-u/r\partial u_i/\partial r+uu_i/r^2]$ are additional terms coming from the derivation of continuum and momentum equations.

Eq. (2.2) is solved in two steps, collision and streaming:

$$\tilde{f}_k(\vec{x},t+\Delta t)=f_k(\vec{x},t)-\frac{1}{\tau_v}\left[f_k(\vec{x},t)-f_k^{eq}(\vec{x},t)\right]+\Delta tF_1+\frac{\Delta t}{6}e_{ki}F_{2i}, \tag{2.3a}$$

$$f_k(\vec{x}+\vec{c}_k\Delta t,t+\Delta t)=\tilde{f}_k(\vec{x},t+\Delta t). \tag{2.3b}$$

In (2.3b), the fictitious particles move to neighbouring nodes, however, in (2.3a) describing the collision steps, particles exchange heat and flow information's (velocities and temperatures), which numerically allows computing new distribution functions according to the old quantities and the relaxation time τ_v. The parameter τ_v and the equilibrium distribution function are written as follows:

$$v=\frac{\tau_v-0.5}{3}\frac{\Delta x^2}{\Delta t}, \tag{2.4a}$$

$$f_k^{eq}=\omega_k\cdot\rho\left(1+\frac{\vec{c}_k\cdot\vec{u}}{c_s^2}+\frac{1}{2}\frac{(\vec{c}_k\cdot\vec{u})^2}{c_s^4}-\frac{1}{2}\frac{\vec{u}\cdot\vec{u}}{c_s^2}\right), \tag{2.4b}$$

where ω_k are directional weighting factors depending on the used lattice Boltzmann model, ρ is the node fluid density, c_s is the lattice sound speed and $\vec{c}_k$ are the directional moving velocities (see Fig. 2), defined as follows:

$$\omega_0=4/9,\quad \omega_k=1/9,\quad k=1,2,3,4,\quad \omega_k=1/36,\quad k=5,6,7,8, \tag{2.5a}$$

$$c_s=c/\sqrt{3}, \tag{2.5b}$$

$$\vec{c}_k=\begin{cases}(0,0), & k=0,\\ (\pm c,0), & k=1,2,3,4,\\ (\pm c,\pm c), & k=5,6,7,8.\end{cases} \tag{2.5c}$$

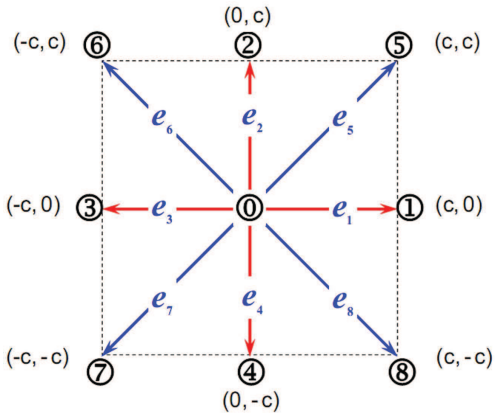

Figure 2: The nine-velocities LB model, D2Q9.

For thermal problems, the thermal LB approach considers two distribution functions, f and g, for the flow and temperature fields respectively; we adopt here the passive scalar approach for its simplicity. Besides, it is well known that the most employed 2D lattice Boltzmann model is the D2Q9 one, used in square lattice. We have found that the D2Q9-D2Q4 is a suitable model for simulating thermal flows, for its stability (compared to D2Q9-D2Q9 model) and to preserve computational effort since the collision process in LBM modeling takes around 70% of the CPU time.

For heat transport, the temperature evolution equation in the four-speed (D2Q4) lattice Boltzmann model is given, for $1\leq k\leq 4$ as:

$$g_k(\vec{x}+\vec{c}_k\Delta t,t+\Delta t)=g_k(\vec{x},t)+\frac{1}{\tau_\alpha}\left[g_k^{eq}(\vec{x},t)-g_k(\vec{x},t)\right]+\Delta t S, \tag{2.6}$$

where $S=\alpha/r\cdot\partial\theta/\partial r$ is considered as a sink term and can be solved by simple FD scheme, g_k^{eq} and τ_α are similarly as discussed above the equilibrium distribution for the temperature field and the corresponding single relaxation time defined as:

$$\alpha=\frac{\tau_\alpha-0.5}{2}\frac{\Delta x^2}{\Delta t}, \tag{2.7a}$$

$$g_k^{eq}=w_k\cdot\theta\cdot\left[1+\frac{\vec{c}_k\cdot\vec{u}}{c_s'^2}\right],\quad c_s'^2=\frac{1}{2}. \tag{2.7b}$$

The macroscopic fluid properties: density, velocity and temperature can be computed as follows:

$$\begin{cases}\text{Flow density}:\ \rho=\sum\limits_k f_k,\\ \text{Momentum}:\ \rho u_i=\sum\limits_k f_k c_{ki},\\ \text{Temperature}:\ \theta=\sum\limits_k g_k.\end{cases} \tag{2.8}$$

2.3 Lattice Boltzmann turbulence modeling

The plasma jet is laminar in its core and turbulent in between fringes due to the high field gradients (200 K/mm and 10 m/s/mm). In LBM-Large Eddy Simulation (LES) modelling of turbulence, only the collision relaxation time is locally readjusted, by adding the eddy viscosity ν_t to the molecular one as:

$$\begin{aligned}\tau_{f\_eff}&=3\nu_{eff}+0.5\\ &=3(\nu+\nu_t)+0.5\\ &=3(\nu+(C_{smag}\Delta)^2|S_{\alpha\beta}|)+0.5,\end{aligned} \tag{2.9}$$

where C_{smag} is the Smagorinsky constant (≈ 0.085), Δ is filter width ($=1$) and $|S_{\alpha\beta}|$ is the strain rate tensor. Eq. (2.9) yields to a quadratic equation in the effective relaxation time

τ_{f_eff} that leads to:

$$\tau_{f\_eff}(x,t)=\left(\tau_v+(\tau_v^2+18\,(C_{smag}\Delta)^2|Q_{\alpha\beta}|/\rho(x,t))^{1/2}\right)/2, \tag{2.10}$$

where $Q_{\alpha\beta}=\sum_k e_{k\alpha}e_{k\beta}(f_k-f_k^{eq})$ and $|Q_{\alpha\beta}|=\sqrt{2Q_{\alpha\beta}Q_{\alpha\beta}}$.

Similarly for the thermal field, the relaxation time is readjusted by using the new thermal diffusivity as:

$$\alpha_{eff}=(\tau_{g\_eff}-0.5)/2=\alpha+\alpha_t=\alpha+\upsilon_t/Pr_t, \tag{2.11}$$

where Pr_t is the turbulent Prandtl number taken here to be 0.45.

2.4 Conversion LB-physical spaces

As mentioned above, argon plasma jet is a high temperature flow. So, that all the thermo-physical plasma properties (viscosity, diffusivity, specific heat, density, sound speed, power radiation$\cdots$) are temperature dependent. The discrete data of these quantities are coded in T&TWinner by [14, 15]. A new special issue in this study is that one must perform conversion between LB and Physical spaces to account for the high temperature-dependence. For general cases, one obtains the same dimensionless value when making dimensionless a quantity φ in LB-space and Ph-space as:

$$\frac{\varphi_{LB}}{LB\_scale}=\frac{\varphi_{Ph}}{Ph\_scale}. \tag{2.12}$$

The table at Fig. 3 summarizes the conversion rules between LB quantities and their corresponding physical values.

DENOMINATION	LBM CONTEXT	PHYSICAL CONTEXT
SPACE STEP	$\Delta x=1$	$\Delta x=L_0/m$
TIME STEP	$\Delta t=1$	$\Delta t=\Delta x\,c_s/C_s$
SOUND SPEED	$c_s^2=1/3$ (FOR D2Q9)	$C_s(T)$
KINETIC VISCOSITY	$\upsilon_{LB}=(\tau_\upsilon-0.5)c_s^2$	$\upsilon_{Ph}=\upsilon_{LB}(C_s/c_s)L_0/m$
THERMAL DIFFUSIVITY	$\alpha_{LB}=(\tau_\alpha-0.5)c_s^2$	$\alpha_{Ph}=\alpha_{LB}(C_s/c_s)L_0/m$
VELOCITY	$\boldsymbol{u}_{LB}=\sum_k \boldsymbol{e}_k f_k/\rho$	$\boldsymbol{u}_{Ph}=\boldsymbol{u}_{LB}\,C_s/c_s$
TEMPERATURE	$\theta=\sum_k g_k$	$T=(T_{\max}-T_{\min})\theta+T_{\min}$

Figure 3: Conversion between LB and physical (real) spaces.

3 Considered configuration

A half plan is considered as a computational domain for the axisymmetric plasma jet. The graph is mapped in Fig. 4, where the nozzle radius R=OA=4 mm, W=OB=12×R, L=OD=100 mm. AB is the anode thickness, then, no-slip boundary condition ($u=0$) and a fix temperature ($T_{\min}=300$K) are retained; BC is a fixed temperature ($T_{\min}=300$K) and a free bound for the velocity ($\partial u/\partial n=0$) is adopted; CD is a boundary that we will describe later; OD is an axisymmetric boundary; OA is governed by the inlet condition of Eq. (3.1):

$$\begin{cases} u_{in}=u_{\max}\left[1-\eta^{a}\right], \\ T_{in}=\left(T_{\max}-T_{\min}\right)\left[1-\eta^{b}\right]+T_{\min}, \end{cases} \tag{3.1}$$

where $u_{\max}$ and $T_{\max}$ are the velocity and temperature of the plasma jet at the torch axis, $T_{\min}$, the temperature of the anode, set to 300K, $\eta=(r/R)$. Parameters a and b give the forms of the inflow conditions. Authors, [16, 17] assume the values subject to the constraints provided by the given values of argon mass flow rate and net torch power. In the present study a flat inlet temperature profile is considered (i.e. $b\equiv\infty$) and "a" is decided hereafter. The initial argon density is set to $\rho=0.027$ Kg/m^3.

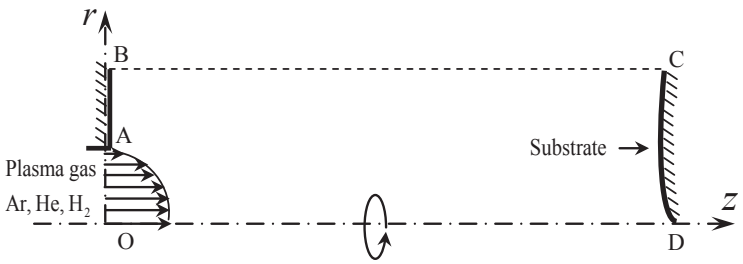

Figure 4: Computational domain.

In simulating and modelling plasma-jets, there is no limitation in the choice of the computational domain, except the typical plasma jet length (spray distance) 100 mm, the plasma jet is observed to be fully developed for about this length. Previous studies are performed for various domain sizes in axial and radial coordinates. In the present study, the domain sizes are as follows: $0\leq z\leq 100$ mm, $0\leq r\leq 48$ mm. An (r,z) to (x,y) transformation is done, so that we solve Eq. (2.1) in Cartesian space [4]. The computational domain is mapped by a uniform mesh. The flow chart of the calculation procedure is sketched in Fig. 5.

4 Results and discussions

In this study, we'll examine the ability of the LB method for treating such complexity. This section, hence, is divided in two parts dealing with argon and argon-nitrogen plasma jets

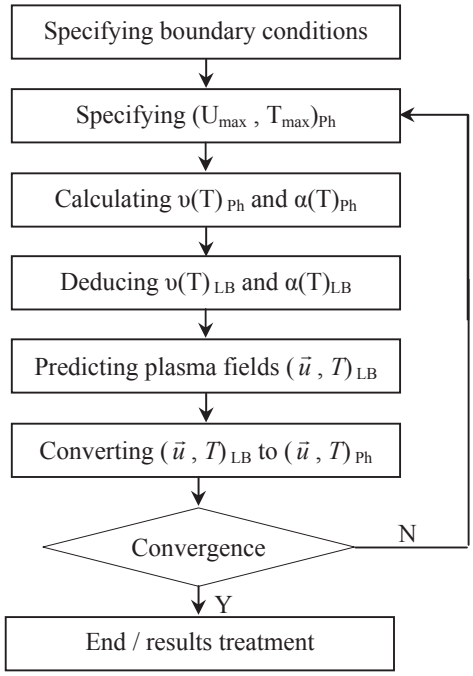

Figure 5: Flow chart of the calculation.

investigations. The plasma gas flow is supposed discharging in an atmosphere of the same gas at 300K.

The LB method has been widely used to study simple jets or jets in simple geometries [18, 19]. However, it is worth mentioning that the jet behaviour depends heavily on boundary conditions. In confined space, the case of Poiseuille flow, the jet takes a parabolic transverse profile that depends on the Reynolds number. For the wall jet the profile is not symmetric; and a Gaussian development takes place in transverse directions. However, for free jets, the transverse profile fields (velocity, temperature,$\cdots$) are Gaussian and the jet is driven by its potential core in all cases. In the computed results in [19] including the distribution of centreline mean-streamwise velocity, the jet spread model shows an excellent agreement with measured and former numerical work and that the LBE is a potentially viable tool for LES turbulence computing.

First, the present study evaluates the ability of LB method to deal with temperature dependent diffusion parameters (viscosity and diffusivity) since temperature variation for thermo-physical quantities is quite smoothed for pure plasma gases than mixed gas ones that present additional peaks at ionization temperatures. Second, we'll demonstrate at what level the LB thermal model account well for plasma physics. In this study, we consider the two cases: with and without substrate. Work-piece constitutes a different boundary condition when spraying in spite of the most widely used, free boundary in plasma jet modelling.

Due to its high heat transfer rates near the stagnation point, impinging jets have been used in many engineering and industrial applications where heating or cooling processes are required. In the case of plasma jets an appropriate and real case study is to consider the working piece as an effective boundary condition. When the jet impinges on the solid boundary, a deflection region and a wall jet region are formed. The behaviour is far from free jet situation. As a consequence, the dynamic and thermal in-flight particles behaviour differs from the case of free jets.

4.1 Pure gas free plasma jets

First of all, a validation analysis based on free jet is done. Therefore, the boundary CD is considered as a free boundary. The present LB results based on the centreline profiles of axial-velocity and temperature (Fig. 6) are compared to available numerical and experimental results of Pfender [1] and the results of the Jets&Poudres code using k-ε turbulent model [20] for specified jet conditions (see [21]).

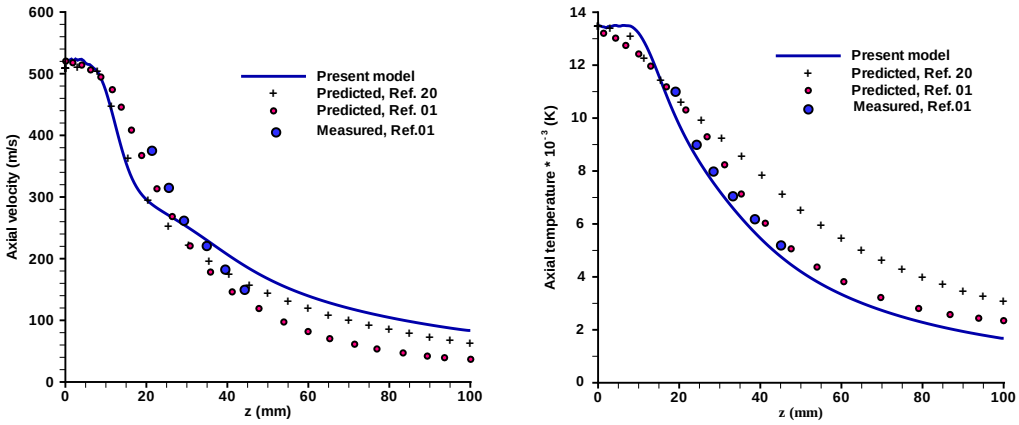

Figure 6: Centerline profiles of the axial velocity (left) and temperature field (right) in comparison with referenced results.

One can remark that the axial temperature gradient near the inlet (interval 0-25 mm) is close to 162 K/mm; which agrees well with the experimental observation (200 K/mm) than Jets&Poudres result (136 K/mm) and Pefender one (152 K/mm). It is the same for the LB velocity gradient which is close to 9.50 (m/s)/mm counter 10.48 (m/s)/mm and 9.48 (m/s)/mm for Jets&Poudres and Pfender results respectively; which agrees well with former experimental and numerical observations as noted here-above. It is, also, clear that our results agree well with Pateyron's ones for the dynamic field and agree with the Pfender's results for the thermal field which gives our results to be a good compromise over the computational plan.

Fig. 7 presents the isotherms and iso-axial velocities of our results for a=2 in Eq. (3.1). It is clear from LB results that the temperature distribution is more expanded than the

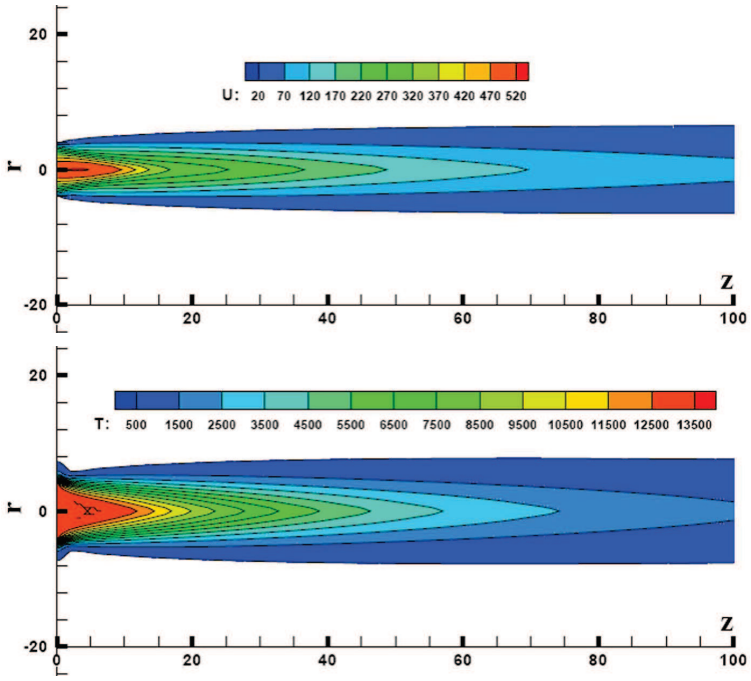

Figure 7: Axial velocity distribution (top) with interval of 50 m/s and temperature distribution (bottom) with interval of 1000K for the present LB model. The unit of variables r and z is the "mm". Negative r-values are reflected about axis $r=0$.

axial-velocity one, and it shares this characteristic with most previous predicted results, where the jet-width does not exceed at all 10 mm for the temperature and velocity distributions. This behaviour, for LB results, is in good agreement with experimental plasma-jet characteristics because plasma jet is more extended, however flame jets are more expanded.

Fig. 8 shows the radial distributions of the analytic and the simulated axial velocity and temperature at different sections from the nozzle exit. The Gaussian profiles for the two fields hold for all the cross sections, the present predictions are found to match well the well-known dimensionless form of the velocity and temperature, these forms are expressed as [22]:

$$\begin{cases} \dfrac{U(r,z)}{U_c(z)} = \exp\left[-\ln(2)\eta_U^2\right], \\ \dfrac{T(r,z)}{T_c(z)} = \exp\left[-\ln(2)\eta_T^2\right], \end{cases} \tag{4.1}$$

where $\eta_\phi = \delta_{0.5}$ is the transverse distance at which $\phi(r,z)/\phi_c(z) = 0.5$ (ϕ stands for U or T and $T_c(z) = T(0,z)$). It is well to mention here, that in the theory of free jets [22], the transverse development of field profiles are modelled by the normalised Gaussian

function centred on zero and expressed as follows:

$$\frac{U(r,z)}{U_c(z)} = \exp\left[-\zeta\left(\frac{r}{z}\right)^2\right], \tag{4.2}$$

where the parameter ζ is linked to the spreading rate S of the jet as $\zeta = \ln(2)/S^2$.

From Fig. 8, one can say that the velocity vectors traces of our simulation match the radial Gaussian distribution, which prove the free boundary condition taken at the north wall in spite of parabolic profiles shown in [23] which matches the non-slip boundary condition. We, also, may mention that velocity vectors traces give idea about convergence time, in our computations we found that convergence time is reached for about 50 times the number of axial grid.

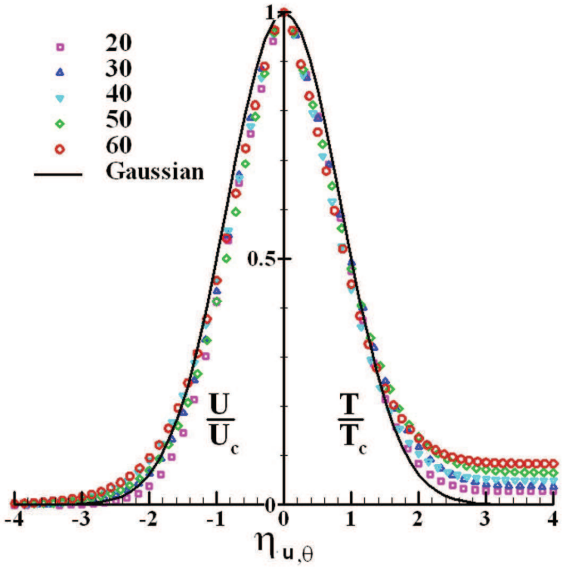

Figure 8: The LB present predictions for the normalized radial temperature and axial velocity profiles for different cross sections in comparison with the Gaussian curve.

4.2 Case with target (substrate)

Spray processes aims to deposit matter on a substrate. On such a way, an important issue in plasma jets modelling is to take account for the target as a fixed boundary condition. Consequently, the flow and thermal structures will be affected by this border effect. The idea is very intuitive for a good (real) prediction of dynamic and thermal history of in-flight particles. The work-piece may have several inclinations with plasma jet axe. The impinging angle is one of several parameters controlling the manner in which a molten or semi-molten particle flattens and solidifies. We just consider here the case of plasma jet impinging normally on the work-piece. The work-piece is a centred flat plate of 48 mm in

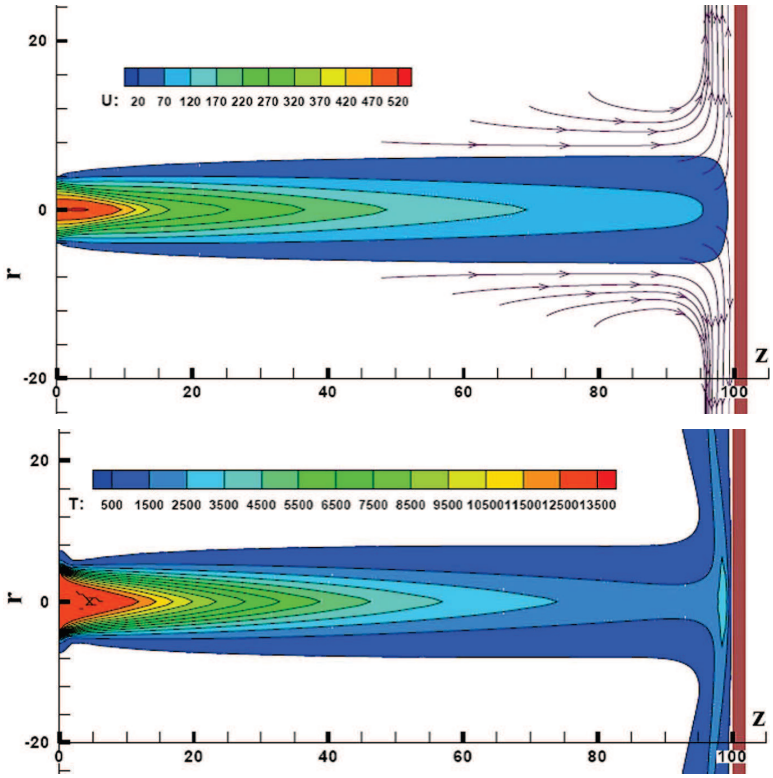

Figure 9: LB results for a normally impinging jet, top: axial velocity distribution with interval of 50 m/s and bottom: temperature distribution with interval of 1kK. The unit of variables r and z is the "mm". Negative r-values are reflected about axis $r=0$.

transverse direction. The non-slip boundary condition and low temperature are retained in our treatment. The target stands 100 mm away from the torch exit. Results show categorical behaviours as depicted in Fig. 9.

Distributions in Fig. 9 are in good agreement with the literature results [24]. The temperature and the axial velocity distributions are flatten locally at the down stream near the work piece. The centreline fields' profiles undergo major variations. The deformation of the jet near work-piece will affect appreciably the sprayed particles trajectories and heating history and particularly its incidence.

4.3 Mixed gas plasma jets

Through this pure argon exercise, the LBM is found to be able to describe efficiently the plasma jet behaviour. However, in plasma spraying it is of great importance to choose the appropriate plasma gas for the spraying material. Then, the mixture gases are used when looking for some jet properties that depend on the volume rates. Conversely, for gas mixture the temperature dependence for the diffusion parameters becomes more complex compared to pure gases ones (smoothed dependence) due to the additional ionization

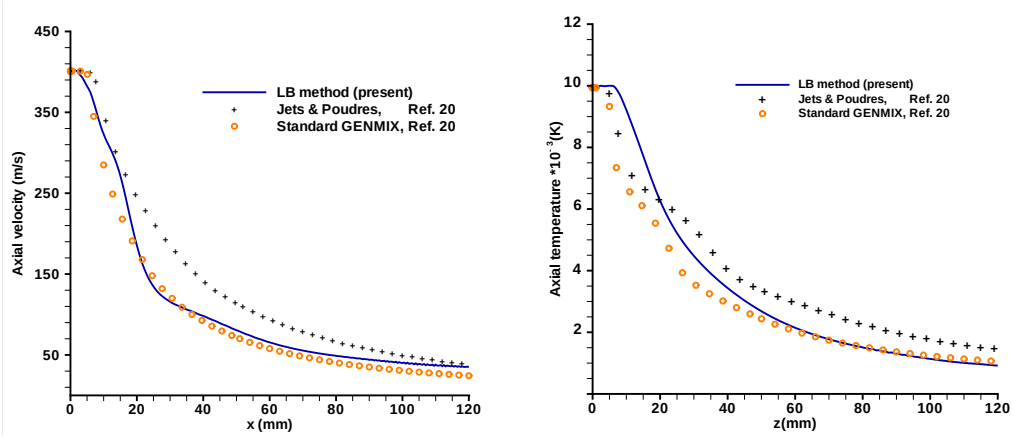

Figure 10: LB predictions for the centerline distribution of the axial velocity (left), and temperature field (right) in comparison with results of Jets&Poudres solver and its standard version GENMIX.

and dissociation temperatures. The LBM will be used in this part to simulate a mixture of gases, namely the argon-nitrogen N_2-Ar62.5% vol. The initializing conditions are $u_{\max}=400$ m/s and $T_{\max}=10000$K, $L=120$ mm and $a=2$.

The LB results are compared with those of Jets&Poudres solver and its standard version GENMIX [20] using mixing-length turbulent model (see Fig. 10) for the same characteristics discussed above for pure argon plasma. As one can see, a good agreement is found with predictions of such codes which use different turbulence model (i.e. the k-ε model). In a more detailed comprehensive study, it has been shown in [25] that all the above discussed properties of pure gas plasma jets (jet width, transverse temperature and in presence of velocity developments, behaviour in presence of target,$\cdots$) are well captured by the present LB modelling.

5 Concluding remarks

In this paper an axisymmetric plasma-jet flowing into stagnant same plasma gas is simulated by using the Lattice Boltzmann method. The turbulent character is modelled and the temperature dependence of diffusion parameters is taken in account leading to important conclusions dealing with the ability of the approach to simulate complex flows; namely axisymmetric turbulent flows with strong temperature dependent physical parameters. It was shown the possible incorporation of the LES turbulence model. On the basis of this LBM numerical study, the following conclusions can be drawn:

- The computed centreline temperature and axial velocity by LB method compare well with available numerical and experimental results of previous studies.
- The temperature and axial velocity distributions are more representative for the axially-extended plasma jet than other available LB-based simulation results.

- The major weak-point of our study is, first, to prove the former Navier-stokes predicted results using the lattice Boltzmann method. That is based on the fact that LBM is particularly adopted for gaseous flows, and its scheme is naturally time-dependent. Second, to develop a new simple model that serves for this class of complex flows (time-dependent, thermal, free jet, turbulent, temperature dependent viscosity$\cdots$);

- The simplicity and accuracy of the method are at the head of its exceptional advantages. It is important to describe accurately the complex fluid flow and interface deformations in a realistic configuration (3D without simplified models) for the first two cases studies. For the plasma jet case study, a good representation of the plasma jet physics results in a good interaction between plasma and in-flight particles (dynamic and heat transfers) and consequently a good agreement with measured results.

This works makes an advance on modelling the plasma jet by using LB approach. On one side the classical results of jet flows are recovered. In other side, the LB has the potential to represent specific physics of plasma. The work progresses on providing a complete description of the plasma particles interaction by using the LB approach, allowing the integration of specific physical properties on the representation of the reactive flow containing flying particles under fast unsteady changes.

Acknowledgments

This work was supported in part by the Ministry of Higher Education and Scientific Research of Tunisia. The first author would like to thank particularly the University of Limoges for the computational facilities provided by CALI calculation centre, and the "Fonds de dotation PERENNE" for financial supports.

References

[1] E. Pfender and C. H. Chang, Plasma spray jets and plasma-particulates interactions: modeling and experiments, Proceedings of the 15th International Thermal Spray Conference, 25-29 May 1998, Nice, France.
[2] G. Mariaux, P. Fauchais, M. Vardelle and B. Pateyron, Modeling of the plasma spray process: From powder injection to coating formation, High Temperature Material Processes, 5(1) (2001), 61-85.
[3] R. Djebali, H. Sammouda and M. El Ganaoui, Some advances in applications of lattice Boltzmann method for complex thermal flows, Adv. Appl. Math. Mech., 2(5) (2010), 587-608.
[4] J. G. Zhou, Axisymmetric lattice Boltzmann method, Phys. Rev. E, 78 (2008), 036701.
[5] S. Hou, J. Sterling, S. Chen and G. D. Doolen, A lattice Boltzmann subgrid model for high Reynolds number flows, in: Pattern Formation and Lattice Gas Automata, A. T. Lawniczak, R. Kapral (Eds.), Fields Inst. Comm., 6 (1996), 151-166.

[6] Y. H. Qian, D. D'Humieres and P. Lallemand, Lattice BGK models for Navier-Stokes equation, Europhys. Lett., 17(6) (1992), 479-484.
[7] A. A. Mohamad, Lattice Boltzmann Method: Fundamentals and Engineering Applications with Computer Codes, Springer Verlag, 2011.
[8] D. Lycett-Brown, I. Karlin, K. H. Luo, Droplet collision simulation by a multi-speed lattice Boltzmann method, Commun. Comput. Phys., 9(5) (2011), 1219-1234.
[9] P. M. Dupuy, M. Fernandino, H. A. Jakobsen and H. F. Svendsen, Multiphysic two-phase flow lattice Boltzmann: droplets with realistic representation of the interface, Commun. Comput. Phys., 9(5) (2011), 1414-1430.
[10] S. Schmieschek and J. Harting, Contact angle determination in multicomponent lattice Boltzmann simulations, Commun. Comput. Phys., 9(5) (2011), 1165-1178.
[11] T. Inamuro, H. Hayashi and M. Koshiyama, Behaviors of spherical and nonspherical particles in a square pipe flow, Commun. Comput. Phys., 9(5) (2011), 1179-1192.
[12] B. He, Y. Chen, W. feng, Q. Li, A. Song, Y. Wang, M. Zhang and W. Zhang, Compressible lattice Boltzmann method and applications, Int. J. Num. Anal. Model., 9(2) (2012), 410-418.
[13] D. Raabe, Overview of the lattice Boltzmann method for nano- and microscale fluid dynamics in materials science and engineering, Modelling Simul. Mater. Sci. Eng., 12 (2004), R13-R46.
[14] E. Meillot, A. Vardelle, J. F. Coudert, B. Pateyron and P. Fauchais, Plasma spraying using Ar-He-H2 gas mixtures, 1st Proceedings of the International Thermal Spray Conference, pp. 803-808, 1998.
[15] B. Pateyron, G. Delluc and N. Calvé, T&TWinner, the chemistry of non-line transport properties in interval 300K to 20000 K, Mécanique et industries, 6 (2005), 651-654.
[16] H.-X. Wang, X. Chen and W. Pan, Modeling study on the entrainment of ambient air into subsonic laminar and turbulent argon plasma jets, Plasma Chem. Plasma Process., 27 (2007), 141-162.
[17] J. D. Ramshaw and C. H. Chang, Computational fluid dynamics modeling of multicomponent thermal plasmas, Plasma Chem. Plasma Process., 12(3) (1992), 299-325.
[18] H. Yu, L.-S. Luo and S. S. Girimaji, LES of turbulent square jet flow using an MRT lattice Boltzmann model, Computers & Fluids, 35 (2006), 957-965.
[19] T. Lee, C.-L. Lin and L.-D. Chen, A lattice Boltzmann algorithm for calculation of the laminar jet diffusion flame, J. Comput. Phys., 215 (2006), 133-152.
[20] B. Pateyron, 'Jets&Poudres' free downlowd from `http://www.unilim.fr/spcts` or `http://jets.poudres.free.fr`
[21] R. Djebali, B. Pateyron, M. El Ganaoui and H. Sammouda, Axisymmetric high temperature jet behaviors based on a lattice Boltzmann computational method Part I: Argon plasma, Int. Rev. Chem. Eng., 1(5) (2009), 428-438.
[22] A. Van Hirtum, X. Grandchamp and X. Pelorson, Moderate Reynolds number axisymmetric jet development downstream an extended conical diffuser: Influence of extension length, Eur. J. Mech. B–Fluids, 28 (2009), 753-760.
[23] H. Zhang, S. Hu, G. Wang and J. Zhu, Modeling and simulation of plasma jet by lattice Boltzmann method, Applied Mathematical Modelling, 31 (2007), 1124-1132.
[24] D. Y. Xu, X. C. Wu and X. Chen, Motion and heating of non-spherical particles in a plasma jet, Surf. Coat. Tech., 171(1-3) (2003),149-156.
[25] R. Djebali, B. Pateyron, M. El Ganaoui and H. Sammouda, Lattice Boltzmann computation of plasma jet behaviors: Part II. Argon-azote mixture, Int. Rev. Chem. Eng., 2(1) (2010), 86-94.